Research article

The molecular and network mechanisms of antilipidemic potential effects of Ganfule capsules in nonalcoholic fatty liver disease

Yu Pan [a,b,1], Liya Qiao [a,c,1], Yunkun Zhang [d,e], Suren R. Sooranna [f], Danna Huang [a,b], Min Ou [a,b], Fei Xu [d,e,***], Lu Chen [a,b,**], Dan Huang [d,g,*]

[a] Guangxi Botanical Garden of Medicinal Plants, Nanning, 530023, Peoples Republic of China
[b] National Engineering Research Center of Southwest Endangered Medicinal Resource Development, Nanning, 530023, Peoples Republic of China
[c] Chinese Medicinal Materials Product Quality Supervision and Inspection Station, 530023, Peoples Republic of China
[d] Hunan Engineering Technology Research Center for Bioactive Substance Discovery of Chinese Medicine, School of Pharmacy, Hunan University of Chinese Medicine, Changsha, 410208, Peoples Republic of China
[e] Hunan Province Sino-US International Joint Research Center for Therapeutic Drugs of Senile Degenerative Diseases, Hunan University of Chinese Medicine, Changsha, 410208, Peoples Republic of China
[f] Academic Department of Obstetrics and Gynaecology, Imperial College London, Chelsea and Westminster Hospital, 369 Fulham Road, London, SW109NH, United Kingdom
[g] State Key Laboratory of Chinese Medicine Powder and Medicine Innovation in Hunan (Incubation), Science and Technology Innovation Center, Hunan University of Chinese Medicine, Changsha, 410208, Peoples Republic of China

ABSTRACT

Background: Non-alcoholic fatty liver disease (NAFLD) is a common liver disorder characterized by hepatic steatosis, inflammation and fibrosis. Ganfule (GFL), a traditional Chinese medicine, has demonstrated therapeutic potential in the treatment of NAFLD but the mechanisms involved are not fully understood.To evaluate the biochemical mechanisms of GFL in treating NAFLD by examining its effects on biological networks, key therapeutic targets, histopathological changes and clinical implications.

Methods: Chemical component screening, key target prediction, biological functional enrichment analysis, lipid profile localization analysis and complex network analysis were performed on GFL using multi-database mining, network analysis and molecular docking. An NAFLD rat model was then established and treated with different doses of GFL. Histopathological evaluation and western blotting were used to verify the expression levels of key target proteins in GFL-treated NAFLD rats.

Results: Network analysis analysis identified 12 core targets, 12 core active ingredients and 7 core Chinese medicinal herbs in GFL potentially involved in the treatment of NAFLD. Biological functional enrichment analysis revealed the involvement of lipid metabolism, apoptosis and

intracellular signaling pathways. Molecular docking confirmed a strong affinity between GFL's core compounds and certain target proteins. Histopathological examination of an NAFLD rat model showed reduced hepatocellular steatosis after GFL treatment. Western blotting revealed significant downregulation of PPARA and PPARD protein expression and upregulation of PIK3CG and PRKACA protein expression in NAFLD rats treated with lower doses of GFL.

Conclusions: Our results suggest that GFL modulates key proteins involved in lipid metabolism and apoptosis pathways. GFL improved the histopathological features of NAFLD rats by regulating lipid metabolism as well as reducing hepatocyte apoptosis and hepatocellular steatosis. These findings offer insights into the biochemical mechanism of action of GFL and support its use in the treatment for NAFLD.

Abbreviations

TCM	Traditional Chinese medicine
NAFLD	non-alcoholic fatty liver disease
NASH	non-alcoholic steatohepatitis
GFL	Gganfule treatment group
GCs	anfule capsules
GFL-LD	low dose of Ganfule
GFL-HD	high dose of Ganfule
NOR	normal diet group
MOD	high fat diet group
GLP-1	glucagon-like peptide-1 receptor
PPAR	peroxisome proliferator-activated receptor
FXR	farnesoid X receptor
PPI	protein-protein interaction network
MCL	markov cluster algorithm
GO	gene ontology
FDR	false discovery rate
HPO	human phenotype ontology
RIPA	radio-immunoprecipitation assay
SDS-PAGE	sodium dodecyl sulfate-polyacrylamide gel electrophoresis
PBS	phosphate buffered solution
PBST	PBS containing 0.05 % Tween-20
DAB	diaminobenzidine
HE	hematoxylin–eosin staining
TUNEL	Terminal deoxynucleotidyl transferase dUTP nick end labeling
TC	total cholesterol
TG	triglycerides
ALT	alanine aminotransferase
AST	aspartate aminotransferase
GEHAT	GFL-efficacy groups–herbal medicines-active compounds-key targets network
PRKACA	cAMP-dependent protein kinase catalytic subunit alpha
PIK3CG	PI3-kinase subunit gamma
PPARA	peroxisome proliferator-activated receptor alpha
PPARD	peroxisome proliferator-activated receptor delta
RMSD	Root Mean Square Deviation Clustering
SHBG	sex hormone-binding globulin
DNAJB1	DnaJ homolog subfamily B member 1
FL-HCC	fibrolamellar hepatocellular carcinoma
HCC	hepatocellular carcinoma

1. Introduction

NAFLD is a common chronic liver disease characterized by fat accumulation in the liver. It is associated with metabolic syndrome, including obesity, diabetes and hypertension [1]. NAFLD can progress from simple fatty liver to non-alcoholic steatohepatitis (NASH), which can lead to fibrosis, cirrhosis and even death [2]. NAFLD is a significant health concern and economic burden, with a prevalence

of 24 % (20–29 %) in the general population. Approximately 20–30 % of NAFLD patients will progress to NASH [3]. Currently, there are no specific drugs for preventing and treating NAFLD. Modern clinical interventions include lifestyle changes as well as drugs such as insulin sensitizers, antioxidants, bile acid drugs, PPAR (peroxisome proliferator-activated receptor) agonists, FXR (farnesoid X receptor) agonists and GLP-1 (glucagon-like peptide-1 receptor) receptor agonists, but these have limited efficacy and safety concerns persist [4].

Traditional Chinese medicine (TCM), has a unique theoretical basis and has accumulated abundant clinical experience that demonstrate advantages and characteristics of multi-target and multi-mechanism treatment for NAFLD [5]. TCM can select appropriate Chinese herbal medicines and formulae based on different TCM patterns guided by pattern differentiation and treatment [6]. TCM treatment for NAFLD mainly focuses on the overall protection of the liver as well as improvement of liver function and metabolic status. Its mechanisms manifest in various forms and features, and aims to improve liver function and metabolic status and either prevent or delay the progression of liver damage and fibrosis [7,8]. The holistic concept of TCM provides a clinical reference value for further exploring the pathogenesis of NAFLD which is a complex metabolic disorder. This contributes to further exploring the scientific connotation of TCM theory and promotes the modernization of TCM.

Previous studies have confirmed that GFL can show a maeked improvement on liver damage caused by various liver diseases such as liver fibrosis, cirrhosis and liver cancer [9,10]. We have previously used UPLC-Q-TOF/MS and metabolomics to identify the key chemical and metabolic components as well as the metabolic pathways involved GFL treatment of liver cancer [11,12]. However, as a multi-drug and multi-component compound Chinese medicine, the efficacy of the bioactive substances, mechanisms of action and targets of GFL in the treatment of NAFLD remain unclear. Therefore, it is necessary to further explore and elucidate the mechanism of action of GFL in the treatment of NAFLD.

Network analysis employs the construction of complex biomolecular networks in order to investigate the systemic mechanisms underlying drug action. This approach offers the advantage of elucidating the holistic effects of drug action, encompassing the mechanisms by which multiple drugs act on multiple targets and the pathways through which drugs can transmit their biological actions [13,14]. In addition. molecular docking technology enables the accurate prediction of binding modes between drug molecules and target proteins [15,16]. This facilitates the rapid screening of compounds with potential therapeutic effects and can provide a crucial guide for optimizing the compatibility of complex compound Chinese medicines in the treatment of NAFLD.

In this study, we employed network analysis and molecular docking techniques to predict the key active components, crucial herbal combinations, and targets of GFL in the treatment of NAFLD. Subsequently, we established a high-fat diet-induced fatty liver rat model to investigate the pathological changes and biochemical markers in NAFLD rats treated with GFL. We verified the mechanism of action of GFL in treating NAFLD from multiple perspectives, including tissue pathology, lipid deposition, hepatocyte apoptosis and predicted protein targets. Our findings provide insights into the therapeutic strategy of using GFL for the treatment of NAFLD and offer a scientific and effective theoretical basis for identifying the clinical compatibility rules and lipid-lowering mechanisms of this TCM. Ultimately, our goal is to enhance the clinical outcomes and prognosis of GFL in the treatment of patients with NALFD.

2. Materials and methods

2.1. Establishment of a small molecule chemical composition library for GFL

The 18 Chinese herbal components of GFL (excluding 3 animal-based ingredients) were categorized according to the TCM principles of their therapeutic effects. The Chinese herbal components were divided into the following effective groups. These were the 'spleen-tonifying and qi-regulating', 'blood-activating and stasis-eliminating' and 'heat-clearing and detoxifying' groups (Supplementary Table 1). Subsequently, these herbal components were uploaded to the Integrative Pharmacology-based Research Platform of Traditional Chinese Medicine (TCMIP) at http://www.tcmip.cn/TCMIP and http://www.tcmip.cn/ETCM [17]. All the chemical components were collected through this platform and a network of herbal attribution was established by using the Cytoscape software 3.10 package.

2.2. Collection of the GFL and NAFLD targets

In order to obtain the targets related to GFL, we first removed any duplicated small molecular chemical components of GFL. Then, we searched for the corresponding candidate target genes associated with these small molecules by using the TCMIP database. Please note that the TCMIP database does not currently include the potential target genes for Coicis Semen (Yiyiren). To identify NAFLD-related target genes, we utilized several databases including DisGeNET (https://www.disgenet.org/), OMIM (https://omim.org/), DrugBank (https://www.drugbank.com/), TTD (https://db.idrblab.net/ttd/), PharmGKB (https://www.pharmgkb.org/) and GeneCards (https://www.genecards.org/). The keywords "Non-alcoholic Fatty Liver Disease; CUI: C0400966" were entered into these databases to retrieve all the target genes associated with NAFLD.

2.3. Protein-protein interaction (PPI) cluster network analysis

To identify key the target proteins for GFL which are involved in the treatment of NAFLD, we performed a Venn diagram analysis to determine the intersection of the target proteins associated with NAFLD as well as the target proteins associated with the components of GFL. This helped us to identify the crucial target proteins for GFL in treating NAFLD. Next, we imported the obtained target proteins into the STRING database (https://string-db.org/) in order to construct a PPI network and this utilized a required score of 0.40 and an

FDR stringency of ≤0.05 to ensure high-confidence of the interactions. We employed the Markov Cluster Algorithm (MCL) to further analyze the PPI network and the MCL inflation parameter was set to 3, which determined the granularity of the clusters within the network. This clustering analysis helped us identify groups of proteins with similar functions and roles in the context of GFL treatment for NAFLD.

2.4. Complex biological function enrichment analysis

The key target genes involved in GFL treatment for NAFLD were uploaded to the Metascape database (http://metascape.org) and the KEGG pathways were utilized for genomic and metabolomic analysis. The Reactome pathways were used for proteomic analysis and gene ontology (GO) enrichment analysis was conducted for functional annotation of the target genes. The key target genes associated with GFL treatment for NAFLD were identified and subjected to further enrichment analysis using the STRING database. This analysis explored the potential association of the target proteins with diseases, human tissue expression, subcellular localization, and HPO (human phenotypes). The obtained biological data were then ranked based on a false discovery rate (FDR) ≤ 0.001. The top 10 enriched biological functions and signaling pathways were then selected and the results were visualized by using a bioinformatics cloud platform (http://www.bioinformatics.com.cn/).

2.5. Construction of a GFL-efficacy group-herbal medicine-active compound-key target (GEHAT) network

In order to construct the GEHAT network, we first analyzed the attribution of the screened unique small-molecular compounds of GFL and their associated key gene targets in terms of medicinal herbs and effective groups. Subsequently, all the data were imported into Cytoscape 3.10 software for complex network topology analysis. In this analysis, we comprehensively selected five important criteria as composite filtering standards: Degree, Betweenness Centrality, Closeness Centrality, Stress and EdgeBetweenness. The criteria for screening involved the following: all the five parameters must exceed the median values of all nodes. These criteria were used to investigate and analyze the key network nodes in-depth.

2.6. Molecular docking and screening

From the network diagram mentioned above, we selected 13 core compounds with a Druglikeness Weight ≥0.5. The 3D structures of these compounds were downloaded from PubChem (https://pubchem.ncbi.nlm.nih.gov) and converted into the desired format using the OpenBabel 2.4.1 software package. For the 22 core target proteins in the network diagram, their 3D crystal structures were obtained from the RCSB PDB database (https://www.rcsb.org/). The selection criteria for the target protein structures were as follows: Homo sapiens, X-ray diffraction and resolution (Å) ≤ 2.5, R-values cutoff were ranging from 0.15 to 0.3. We then identified the small molecular ligands which had co-crystallized structures with the target proteins. Next, using the Autodocking Tools 1.5.6 software, the structures of all small molecular ligands were subjected to energy minimization, force field application and conformational optimization. The receptor structures were prepared by adding hydrogens, assigning charges, removing water molecules and modifying the amino acid residues. For the geometry optimization of the ligand, we utilized the Root Mean Square Deviation Clustering (RMSD) analysis method, setting an RMSD threshold of 2 Å and a cluster count of 10 to reduce computational load during docking and enhance prediction accuracy. In the ligands-targets protein docking process, the CHARMM scoring function was employed to evaluate ligand-protein binding energy, facilitating the determination of the optimal conformation [18,19]. The potential active pockets and binding sites of the target proteins were determined, and molecular docking calculations were performed in order to screen for small molecule ligand-protein complexes with good affinities. Finally, the Discovery Studio Client 4.4 software was used to visualize the best conformations of the ligands-target protein complexes.

2.7. Preparation of GFL

GFL capsules (GCs) were obtained from Hunan Kangpu Pharmaceutical Co. Ltd. (Changsha, China; specification: 0.5g/capsule; z20060389). According to the recommended daily dosage for adults of GFL capsules, which is 9 g/day (18 capsules/day), the equivalent dosage for rats is calculated as 9g/70 kg × 6.3 = 0.81 g/kg. The capsule contents were thoroughly pulverized, and then dissolved in 0.9 % NaCl solution and ultra-sonication was used to prepare two suspension formulations: one with a concentration of 0.081 g/mL representing a low dose of GFL (0.81 g/kg, GFL-LD), and the other with a concentration of 0.162 g/mL representing a high dose of GFL (1.62 g/kg, GFL-HD). The prepared GFL suspensions were protected from light and stored at −20 °C until use.

2.8. Animals and GFL administration

A group of 28 adult male Sprague Dawley rats (SPF grade) with good health were acquired from the Hunan Slack Jingda Laboratory Animal Co. Ltd. The rats weighed between 220 and 280g (6 weeks old). The laboratory animal production license number of the supplier was SCXK (E) 2018-0104. The rats were individually housed in cages at the Animal Center Laboratory of Wuhan Myhalic Biotechnology Co., Ltd. and maintained at the temperature range of 24–26 °C and a humidity level of 50 %–70 %. The animals were exposed to a natural light/dark cycle. During the acclimation period, which lasted for 3 days, they were allowed unrestricted access to distilled water and the rats were provided with a standard diet to allow them to adapt to the laboratory environment. All experimental procedures conducted in this study were approved and these carried out in strict adherence to the guidelines provided by the local

Institutional Animal Experimentation Ethics Committee (approval number: HLK-20210315-001).

The above rats were randomly divided into four groups: control (NOR), model (MOD), GFL-LD (0.81 g/kg) and GFL-HD (1.62 g/kg). The high fat diet were purchased from Jiangsu Medisen biological medicine Co., Ltd (#MD12033, Nanjing, China). A rat model of NAFLD was induced by feeding a high-fat diet. Seven rats were randomly assigned to the NOR, while the remaining 21 rats were allocated to the NAFLD model group for further experimentation. Following a 24-h fasting period, the rats were intraperitoneally injected with 0.03 g/kg of 3 % pentobarbital sodium (cat. #57-33-0, Shanghai, China) for anesthesia. The NOR and MOD groups received an intragastric administration of 0.1 mL/10 g of 0.9 % NaCl solution, whereas the GFL-LD and GFL-HD groups were orally gavaged with 0.1 mL/10 g of GFL suspensions, with concentrations of 0.081 and 0.162 g/mL, respectively. After a 14-day modeling period, two rats were randomly selected from both the NOR and MOD groups for anatomical observations. The presence of pathological inflammatory changes observed in the liver tissues of the MOD rats indicated the successful establishment of the model.

2.9. Blood lipid assay

Following a 4-week period of gastric gavage in the rats, blood samples were obtained from the abdominal aorta. Intraperitoneal anesthesia was induced using 3 % pentobarbital sodium. The collected blood samples were allowed to clot at room temperature for 30 min to 1 h. Subsequently, centrifugation was performed at 1000–2000 rpm for 20 min in order to separate the sera from the clots and cells. The serum samples were carefully transferred into new tubes using sterile techniques and stored at 4 °C. Upon thawing the rat serum samples at 4 °C, the levels of biochemical markers such as total cholesterol (TC), triglycerides (TG), alanine aminotransferase (ALT), aspartate aminotransferase (AST) and the LDL-C/HDL-C ratio in the liver tissues of SD rats from each group were assessed using an automatic biochemical analyzer (BS-420) manufactured by Mindray (Shenzhen, China). The detection reagents used were provided by Mindray's as a biochemical reagent kit (Shenzhen, China).

2.10. Histopathology of tissues

The rat liver tissues were washed with chilled physiological saline to remove excess blood and impurities. They were then cut into 20 mg pieces and treated with radio-immunoprecipitation assay (RIPA) cell lysate (#R0010, Solarbio, China). Ultrasonic processing was employed to disrupt the cells and release proteins. Centrifugation was performed to remove debris, and the supernatants were discarded. Isopropanol (cat. #67-63-0, Hushi, Shanghai, China) was added to the samples and these were mixed and cryopreserved at −20 °C. The liver morphology, including the weight, shape, color and texture was observed, and the liver weight index (liver wet weight/volume × 100 %) was calculated.

The rat liver tissues were fixed in a 4 % neutral formaldehyde solution for 24 h. After fixation, they were dehydrated in ethanol (cat. #64-17-5, Hushi, Shanghai, China), embedded in paraffin and then cut into 3 μm slices. The slices were dewaxed using xylene (cat. #1330-20-7, Hushi, Shanghai, China), rehydrated with graded ethanol (80 %–95 %) for 15–30 s each, stained with hematoxylin (#G1140, Solarbio, Shanghai, China) for 3–6 min, followed by staining with 0.5 % eosin for 2–3 min. The slices were then washed with ethanol, clarified and cleared in xylene. Finally, the slices were sealed with neutral gum and observed under a Leica DM2700 M upright microscope (Shanghai, China). In order to quantify the size of lipid deposits in the aortic sinus, we applied a solution of Oil Red O (#BA4081, Zhuhai, China) to frozen slices. The solution was diluted at a 3:2 ratio of isopropanol to ddH$_2$O and this was applied at a temperature of 37 °C for 30 min. Subsequently, the slices were counterstained for 2 min.

2.11. Terminal deoxynucleotidyl transferase dUTP nick end labeling (TUNEL)

After conventional dewaxing, the rat liver tissue slices were treated with a 3 % peroxidase inhibitor and incubated at room temperature for 10 min. Subsequently, they were washed three times with deionized water. Following this, the slices were subjected to a 37 °C incubation with protease K for 30 min in a wet box and flushed twice with phosphate-buffered saline (PBS). The TUNEL reaction solution was then applied to the slices and incubated in a wet box at 37 °C for 60 min, followed by three rinses with PBS. To visualize the TUNEL-positive cells, the slices were developed with diaminobenzidine (#DA1010, Solarbio, China) for approximately 10 min, and then washed three times with PBS. Hematoxylin (#G1140, Solarbio, China) double staining was then performed, and subsequent steps involved dehydration, transparency and sealing with a film. TUNEL-positive cells were identified under a microscope as those exhibiting brown-yellow granules within the nucleus.

2.12. Western blotting

The rat liver tissues were lysed using RIPA lysis buffer supplemented with total protease and phosphatase inhibitors. Sodium dodecyl sulfate-polyacrylamide gel electrophoresis (SDS-PAGE) was performed for western blotting using a PAGE Gel Fast Preparation Kit (Shanghai Epizyme Biomedical Technology Co., Ltd, Shanghai, China). The primary antibodies used included PPARA (1:1000, #PAB45611, Bioswamp, Wuhan, China), PPARD (1:1000, #PAB34149, Bioswamp, Wuhan, China), PIK3CG (1:2000, #PAB42067, Bioswamp, Wuhan, China), PRKACA (1:500, #PAB36705, Bioswamp, Wuhan, China) and GAPDH (1:1000, #PAB36269, Bioswamp, Wuhan, China). The proteins were separated by electrophoresis on SDS-PAGE Bis-Tris gels in two stages: 80 V for 40 min and 120 V for 50 min. Following electrophoresis, the proteins were transferred onto nitrocellulose membranes and these were then blocked with 5 % skimmed milk at 4 °C for 1.5 h. Subsequently, the membranes were incubated with the respective primary antibodies for 1 h and then washed three times for 10 min each with PBS containing 0.05 % Tween-20 (PBST, #T8220-100, Solarbio, China). Next, the membranes

were incubated with HRP-labeled goat anti-rabbit IgG secondary antibodies (1:20000, #SAB43714, Bioswamp, Wuhan, China) in PBS for 1 h at 37 °C. Following another round of washing, the target bands were detected using an automated chemiluminescence analyzer (Tanon-5200, Shanghai, China). The optimal antibody dilutions were determined using dilutions ranging from 1:50 to 1:2000.

2.13. Statistical analysis

Statistical analysis was conducted using GraphPad Prism version 8.0.2 software. The Shapiro-Wilk test was used to assess the normality of the data. Group comparisons were performed using either one-way analysis of variance (ANOVA) or the Kruskal-Wallis H test. The measured data are presented as means ± standard deviations. $P < 0.05$ was considered to be statistically significant.

3. Results

3.1. Screening of chemical components in GFL

When screening the chemical components in GFL, it was found that the "spleen-invigorating and qi-regulating" group of compounds consisting of 9 traditional Chinese medicines, were the most effective among the three functional groups. This was comprised of 424 different chemicals, accounting for 52.6 % of the total composition. The "activating blood circulation and resolving stasis" and "clearing heat and detoxifying" groups, each consisting of 4 medicines, contained 207 and 175 chemical components, accounting for 25.6 and 21.7 % of the total composition, respectively. 252 unique chemical components involved in the treatment of NAFLD were selected from these three functional groups (Fig. 1) These comprised mainly of fatty acids, phenolic compounds, anthraquinones, flavonols and plant sterols. Among these chemical components, 18 were identified as key nodes in the GFL-functional group-chemical component network. Among them, sitosterol, stigmasterol, caproic acid, cetylic acid, caprylic acid and catechin were identified as core network nodes and were derived from different medicinal herbs. Codonopsis Radix (Dangshen with 11 compounds), Bupleuri Radix (Chaihu with 11 compounds), Artemisiae Scopariae Herba (Yinchenhao with 7 compounds) and Poria (Fuling with 3 compounds) had the highest contributions in the network. These four herbs shared at least 3 different chemical components.

3.2. Analysis of core network targets in NAFLD treatment with GFL

From the DisGeNET, OMIM, DrugBank, PharmGKB, GeneCards and TTD databases, a total of 140, 7, 232, 1, 288 and 0 unique target
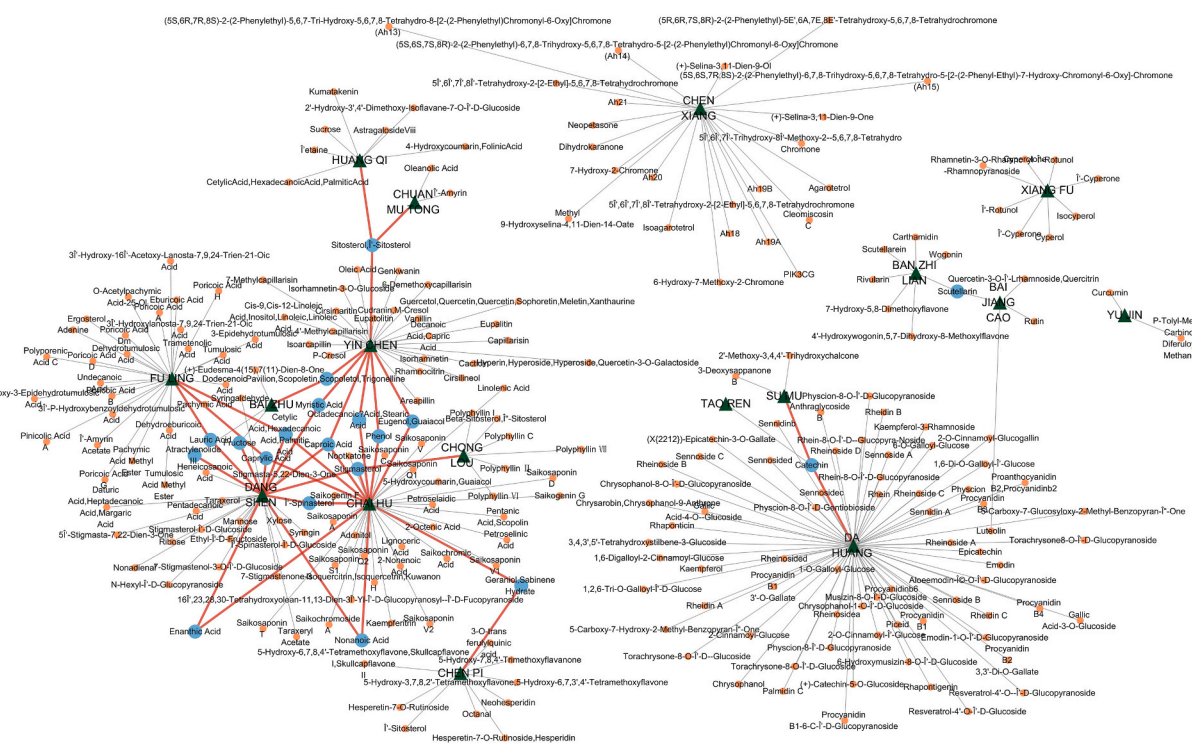

Fig. 1. A network analysis of the chemical components attributed to GFL in the treatment of NAFLD. The network consists of various nodes representing different elements of GFL. The green triangular and blue and brown circular nodes represent the botanical source medicines, key active ingredients and small molecular compounds respectively associated with GFL's treatment of NAFLD. The red edges in the network indicate the connections between the key botanical medicines and the active ingredients, highlighting their critical positions in the network.

genes were obtained, respectively. After merging and removing duplicates, 617 NAFLD-related target genes were identified. Further screening based on clinical indicator scores resulted in a set of 139 high-scoring NAFLD target genes. The intersection of these genes with the 501 target genes of GFL confirmed the presence of 28 potentially active NAFLD targets for GFL (Fig. 2A and B). The results of PPI network clustering analysis revealed that the entire network consisted of 11 edges, with an average node degree of 8.29 and an average local clustering coefficient of 0.643 (Fig. 3). With the exception of NCAN and FOLR2, which may not have direct connections, the other 26 target genes formed three highly interconnected protein subnetworks. Clusters 1, 2 and 3 consisted of 10, 9 and 7 target genes, respectively. Topological analysis of these network targets revealed that ALB, CYP2E1, TNF, IL6, PPARA, AHR, PPARG, SREBF1, IL1B, NR1H4, TLR4 and NQO1, with degrees ≥10, played important bridging roles within the PPI network. These 28 target genes had the highest number of connections to other nodes, indicating their significant contribution to the PPI network as being core nodes.

3.3. Biological functional enrichment analysis of GFL in NAFLD treatment

The GO biological process enrichment analysis revealed that the 28 potential gene targets associated with GFL treatment of NAFLD were primarily involved in the positive regulation of small molecule lipid metabolism (Fig. 4B). These targets actively participate in biological processes related to the metabolism of organic cyclic compounds, particularly those containing oxygen and nitrogen. It was also observed that the receptor complexes formed by these targets may activate nuclear receptors, leading to the modulation of cellular physiological and biochemical responses. Furthermore, the binding of small lipid molecules such as carboxylic acids and fatty acids plays a role in mediating these processes. The KEGG and Reactome pathway analyses provided insights into the pathways influenced by the 28 potential gene targets in GFL treatment of NAFLD (Fig. 4A). The results highlighted the involvement of these targets in insulin resistance and cancer pathways. Specifically, they were found to modulate drug metabolism pathways in the liver by activating cytochrome P450 enzymes. Additionally, the pathways associated with lipid metabolism, including oxidative reactions, steroid metabolism, PPARA activation of gene expression, nuclear receptor transcription, assembly and remodeling of plasma lipoproteins and clearance pathways, were found to be significantly influenced by GFL treatment. These pathways are likely contribute to the regulation of lipid balance in NAFLD. Further analysis revealed that several target proteins, including AHR, PPARA, PPARD, IL1B, IL6, TNF and SREBF1, play crucial roles in the majority of the aforementioned biological processes and signaling pathways. These proteins act as important links within the PPI network and have a high degree of connectivity with other nodes, indicating their central roles in the network. The identified pathways and key target proteins can serve as essential references for further investigations and the development of novel therapeutic strategies for the treatment of NAFLD.

3.4. Lipid profile localization analysis of GFL in NAFLD treatment

Analysis using the STRING database revealed that the 28 potential gene targets associated with GFL treatment of NAFLD are closely related to metabolic disorders, gastrointestinal system diseases and nonalcoholic steatosis hepatitis. Furthermore, NAFLD may also have certain associations with pulmonary edema and pneumonia, which could be attributed to the chronic inflammatory status and immune dysfunction that accompanies this disease. Additionally, the potential key target genes involved in GFL treatment of NAFLD are highly likely to have elevated expression levels in the liver, digestive glands, peritoneal macrophages and Kupffer cells within the human body (Fig. 4C). Subcellular localization analysis suggests that the intracellular mechanisms of GFL treatment in NAFLD involve various receptor complexes, including the NF-κB, nitric oxide synthase, interleukin-23, interleukin-12 and transforming growth factor β complexes (Fig. 4D). Furthermore, phenotype prediction analysis indicates that the therapeutic effects of GFL in NAFLD would require the evaluation of various indicators such as LDL-C, TC and blood lipid levels as well as cardiovascular parameters. These indicators can help to validate the efficacy of GFL in NAFLD treatment in subsequent animal experiments.

3.5. Analysis of GFL's complex biological network in NAFLD treatment

The PPI network's Cluster 1 (PPARA, PPARD, PPARG, PRKACA, PRKCA and SREBF1) within the GEHAT network appears to play a
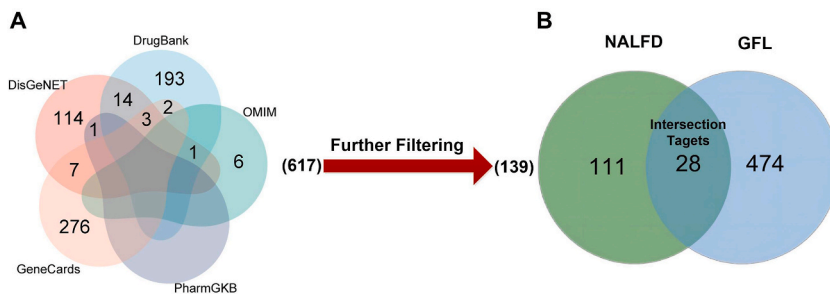

Fig. 2. A Venn diagram illustrating the identification of NAFLD targets. (A) The intersection genes related to NAFLD was obtained from different databases and 617 unique candidate NAFLD target genes were obtained. (B) The intersection of NAFLD target genes with GFL target genes were depicted. Among the set of 502 GFL target genes, 28 genes were found to intersect with the NAFLD target genes.
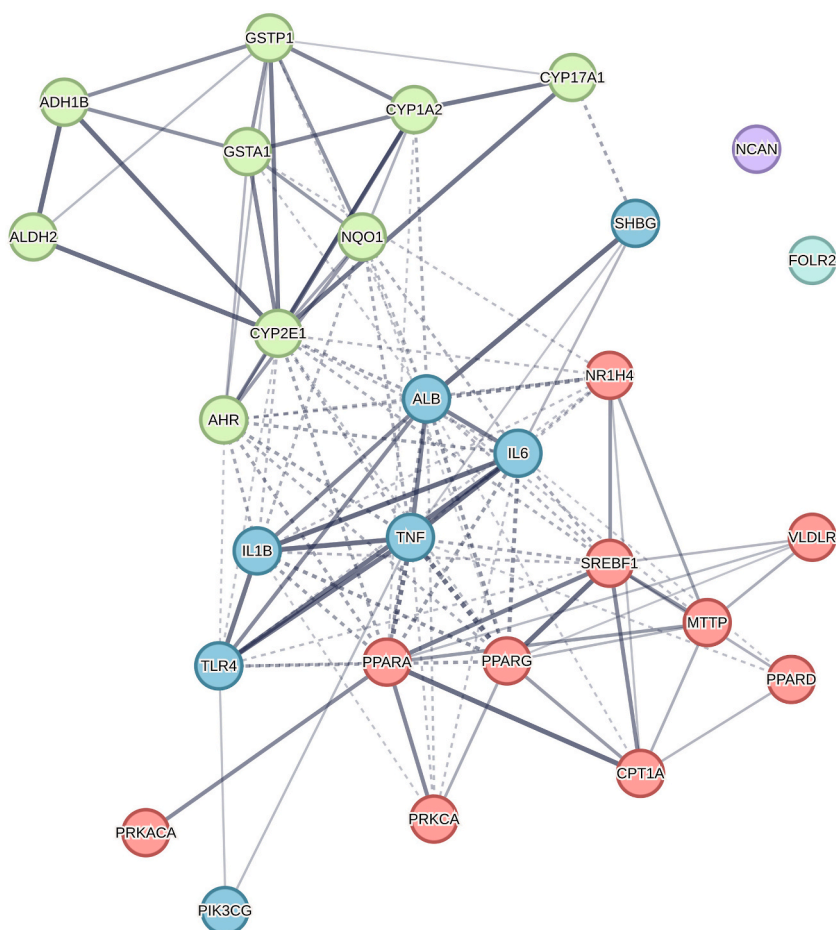
Fig. 3. A cluster analysis of the interaction relationships among the 28 potential targets of GFL in the context of NAFLD using the PPI network. In the network, Clusters 1, 2 and 3 are represented the red, indigo and green nodes, respectively. The strength and thickness of the lines connecting the nodes reflect the degree of closeness between the targets. The filtering criteria used for this analysis were as follows: required score: 0.40, FDR stringency ≤0.05, and MCL inflation parameter = 3.

critical role in GFL treatment of NAFLD. In addition to Cluster 1, the target genes ALB, IL1B, IL6, PIK3CG, SHBG, TLR4 and TNF from Cluster 3 also demonstrated substantial contributions within the GEHAT network (Fig. 5). Therefore, these 13 target genes were considered to be the most likely therapeutic targets of GFL in the treatment of NAFLD (Supplementary Table 2). Furthermore, we identified 19 active compounds with the highest densities in the network, which are probably the key pharmacological components of GFL in the treatment of NAFLD (Table 1). Additionally, the components from the Chinese medicinal herbs Dahuang (Rhei Radix et Rhizoma), Chaihu, Yinchenhao, Fuling, Dangshen, Huangqi (Astragali Radix) and Chenxiang (Aquilariae Lignum Resinatum) occupy central positions in the network. They exhibit high connectivity with other nodes, connect with a significant number of active compounds, bridge most of the key target genes and are closely related to the therapeutic effects guided by TCM principles. Therefore, these herbs are highly likely to be the core components of GFL in the treatment of NAFLD.

3.6. Molecular docking of the GFL core components and the NAFLD targets

To further validate the activities of the 19 core compounds identified from the complex biological network and their docking conformations with the 13 core target proteins, we conducted protein affinity tests using 13 of the key compounds with a Druglikeness Score ≥0.5 (Supplementary Table 3). It is generally accepted that a binding energy of ≤ -4.25 kcal/mol indicates a significant binding activity between a small ligand molecule and its protein receptor [20]. The results revealed that the 13 ligand molecules exhibited favorable binding affinities with the five protein receptors, PPARA, PPARD, PRKACA, PIK3CG and SHBG (Fig. 6A–O). Eugenol, nonanoic acid, geraniol and lauric acid exhibited binding energies of ≤ −5.0 kcal/mol with the aforementioned five protein receptors. Scutellarin and atractylenolide III demonstrated binding energies of ≤8.0 kcal/mol with PRKACA, PPARA, SHBG and PPARD protein targets, indicating strong binding activities. Specifically, scutellarin exhibited a binding energy of −9.2 kcal/mol with PPARD, forming hydrogen bonds with the amino acid residues THR, ASN, and ALA on the oxygen moiety of the furan ring. Atractylenolide III, with its
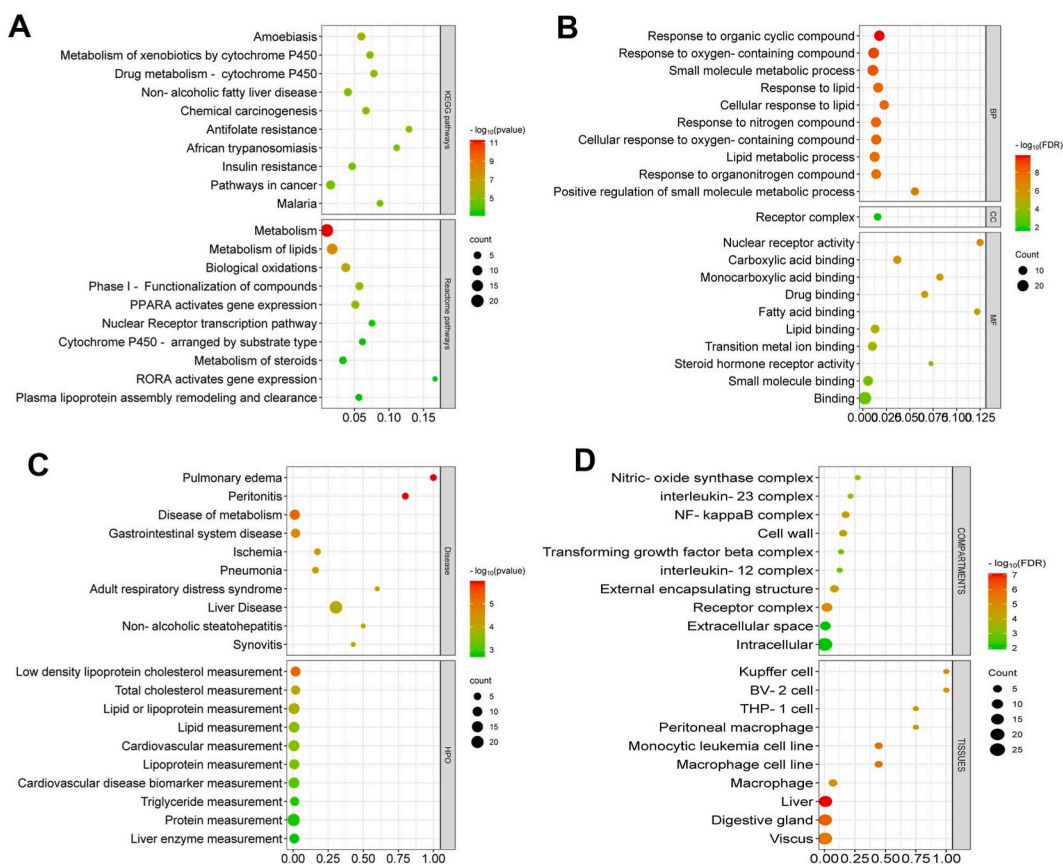
Fig. 4. The functional characteristics and associations of the 28 target genes of GFL in the treatment of NAFLD. (A) The enrichment analysis of associated signaling pathways and metabolic pathways shows the pathways that are significantly associated with the target genes. (B) The biological functional enrichment analysis focuses on the biological functions related to the target genes. (C) The diseases and their corresponding HPO terms associated with the target genes. (D) The compartments and tissues analysis identified the cellular compartments and specific tissues where the target genes are predominantly expressed.

coumarin benzene ring structure, formed hydrogen bonds (binding energy: −8.6 kcal/mol) with the LYS amino acid residue of PPARA through the CO bond on the furan ring, and exhibited pi-alkyl hydrophobic interactions with amino acid residues such as LEU, MET, ALA, PHE and VAL. Catechin showed the lowest binding energy (−9.2 kcal/mol) with SHBG, and its phenanthrene furan ring skeleton formed hydrogen bonds with the amino acid residues THR, SER, VAL and GLY through multiple phenolic hydroxyl groups, indicating a strong binding activity (Fig. 7A–O).

3.7. GFL improves liver morphology and blood lipid levels in NAFLD rats

In this study, we investigated the effects of low and high doses of GFL on liver morphology and blood lipid levels in rats with NAFLD (Figs. 8–9). The NOR group displayed individual traits characterized by shiny and smooth fur, and their livers exhibited a vibrant red color, firm texture and sharp edges. In contrast, animals in the MOD group showed an enlarged body size, disheveled and dull fur, yellowish coat color and significant weight gain ($P < 0.01$). The livers of those in the MOD group exhibited a significant increase in volume, wet weight and liver weight index ($P < 0.01$). Additionally, the livers appeared pale and greasy, with mottled patterns and rounded edges. However, treatment with GFL resulted in noticeable improvements in liver morphology. The GFL-LD and GFL-HD groups showed reduced liver greasiness and a more significant improvement in the liver weight index ($P < 0.05$). In particular, rats in the GFL-LD group exhibited glossy fur, reduced greasiness and restored liver color and texture. Furthermore, compared to the NOR group, the MOD group of rats exhibited a significant increase in TG and TC levels ($P < 0.01$). The activities of ALT and AST were significantly elevated ($P < 0.01$). LDL-C levels showed a marked increase, while HDL-C levels were significantly reduced ($P < 0.01$). However, treatment with in both GFL-LD and GFL-HD groups led to significant improvements in various lipid parameters ($P < 0.01$) compared with the MOD group. Interestingly, the GFL-LD group exhibited the most significant improvements in blood lipid profiles ($P < 0.01$). These findings suggest that GFL has the potential to ameliorate liver morphology and positively influence blood lipid levels in rats with NAFLD, highlighting its therapeutic value in the management of this condition.
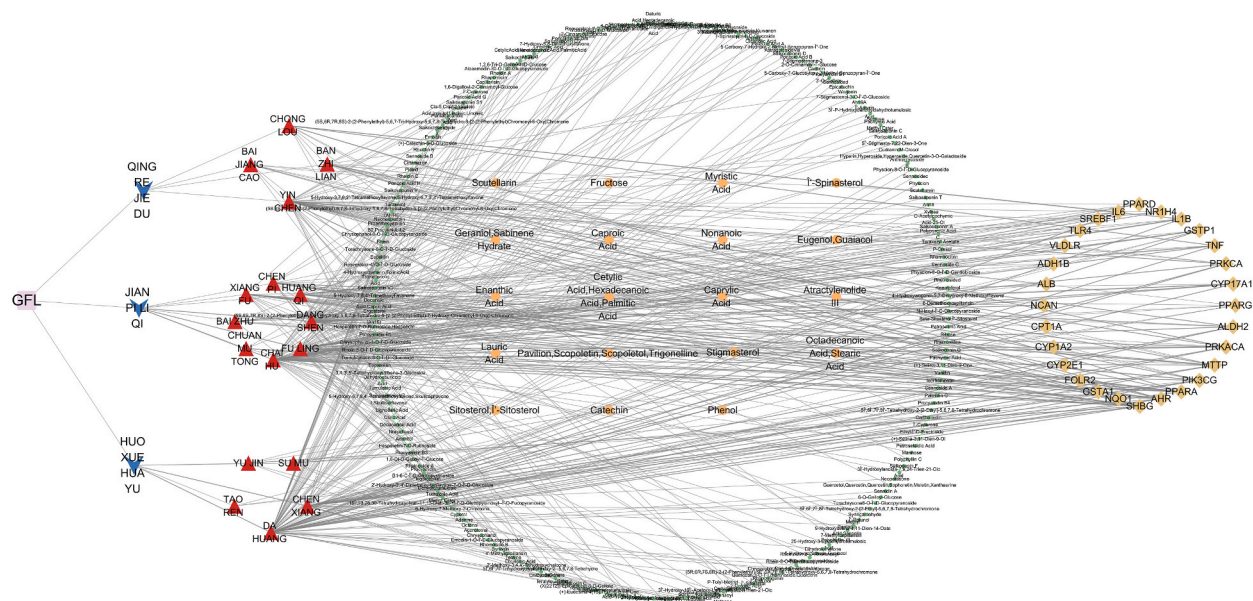
Fig. 5. The network of GFL, Chinese herbal medicines, chemical components and intersection targets. The blue triangular, red inverted triangular and light brown diamond-shaped nodes represent the TCM efficacy groups, the combinations of Chinese herbal medicines and the 28 target genes respectively associated with GFL treatment of NAFLD. The large brown node at the center green and the circular central node represents the 19 critical compounds and all the 252 compounds of GFL respectively associated with the treatment of NAFLD.

3.8. GFL alleviates lipid deposition in NAFLD rats

Histological analysis after H&E staining revealed that the liver lobular structures of rats in the NOR group appeared intact, with clear boundaries and normal hepatic sinusoids. The hepatocytes were polygonal, without any signs of lipid degeneration and other pathological changes. In contrast, compared to the control group, the liver cells of the MOD group showed cellular swelling, cytoplasmic looseness and the presence of variable-sized lipid vacuoles scattered throughout the liver. However, treatment with both low and high doses of GFL significantly improved the tissue structure of liver cells. Animals in both the GFL-LD and the GFL-HD groups exhibited a notable reduction in lipid droplets within the hepatocytes, indicating an improvement in cellular morphology and a marked decrease in lipid deposition when compared to the MOD group (Fig. 10).

Additionally, oil red O staining results showed that the liver cells of rats in the NOR group displayed no formation of red lipid droplets. The cellular structure of the liver was intact and clear, with the nuclei stained blue and no orange-stained lipid droplets were observed in the cytoplasm. In contrast, when compared to the control group, the liver cells of the MOD group exhibited disrupted cellular structures, with abundant red lipid droplets indicating significant lipid deposition. However, when compared to the MOD group, both the GFL-LD and the GFL-HD groups showed significant reductions in the number of round, orange-stained lipid droplets within the liver cells. In particular, the GFL-LD group exhibited the most significant alleviation of lipid deposition in hepatocytes (Fig. 10). These results suggest that GFL has the potential to mitigate lipid deposition and improve liver cell morphology in NAFLD rats, highlighting its therapeutic effects in addressing the lipid accumulation associated with NAFLD.

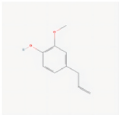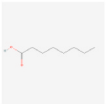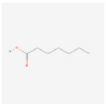### 3.9. GFL has the potential to alleviate apoptosis in NAFLD rats

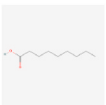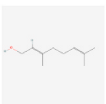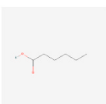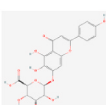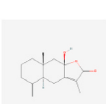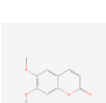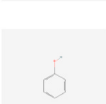The results of TUNEL demonstrated that the liver tissue of rats in the normal diet group exhibited minimal brown staining, indicating low levels of apoptosis. In contrast, the model group of rats showed a significant increase in brown apoptotic cells in the liver tissues when compared to the normal group. However, treatment with GFL significantly reduced the number of brown apoptotic cells in the liver tissue of NAFLD rats. In particular, the rats in the GFL-LD group exhibited the most significant reduction in liver cell apoptosis levels. These findings suggest that GFL has the potential to alleviate apoptosis in NAFLD rats (Fig. 10).

3.10. GFL can modulate the expression levels of key target proteins

In order to validate the predicted target proteins results from molecular docking and network pharmacology analysis, we further investigated the effects of GFL on the expression levels of PPARA, PPARD, PIK3CG and PRKACA. These proteins were shown to be involved in the lipid and apoptotic mechanisms in the liver of NAFLD rats. When compared with the NOR group, treatment with GFL-HD resulted in the downregulation of PPARA and PPARD protein expression ($P < 0.05$) and upregulation of PIK3CG protein expression ($P < 0.05$). When compared to the MOD group, animals in the GFL-LD group had upregulated expression levels of PPARA and PPARD
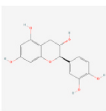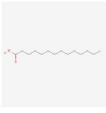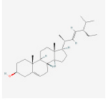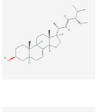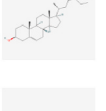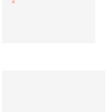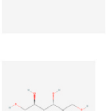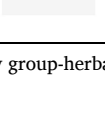
Table 1
The core active ingredients of GFL for the treatment of NAFLD as determined by the GEHAT network.

Compound	Molecular structure	Degree	Between-ness Centrality	Closeness Centrality	Stress	Drug-likeness Weight	Herb
Eugenol		2	0.001096527	0.298298298	2304	0.696	Coicis Semen Bupleuri Radix
Caprylic Acid		3	0.004500068	0.314014752	6916	0.622	Codonopsis Radix Bupleuri Radix Poria
Enanthic Acid		2	0.00112741	0.296517413	2168	0.62	Bupleuri Radix Codonopsis Radix
Nonanoic Acid		2	0.00112741	0.296517413	2168	0.617	Bupleuri Radix Codonopsis Radix
Geraniol		2	9.66E-04	0.287922705	1040	0.617	Bupleuri Radix Citri Reticulatae Pericarpium
Caproic Acid		3	0.004111923	0.313354364	6778	0.608	Bupleuri Radix Codonopsis Radix Coicis Semen
Scutellarin		2	9.30E-05	0.261633011	64	0.598	Scutellariae Barbatae Herba Herba Patriniae
Lauric Acid		2	0.001794524	0.290731707	2096	0.561	Codonopsis Radix Poria
Scopoletin		2	4.97E-04	0.280867107	678	0.542	Coicis Semen Atractylodis Macrocephalae Rhizoma
Atractylenolide III		2	2.53E-04	0.27618165	408	0.529	Codonopsis Radix Atractylodis Macrocephalae Rhizoma
Phenol		2	0.001096527	0.298298298	2304	0.517	Bupleuri Radix Coicis Semen

Table 1 (*continued*)

Compound	Molecular structure	Degree	Between-ness Centrality	Closeness Centrality	Stress	Drug-likeness Weight	Herb
(+)Catechin		3	0.001365643	0.300100705	978	0.514	Rhei Radix et Rhizoma Sappan Lignum Persicae Semen
Myristic Acid		2	0.001887987	0.293018682	2306	0.48	Codonopsis Radix Coicis Semen
Stigmasterol		3	0.003900532	0.301314459	4212	0.46	Codonopsis Radix Bupleuri Radix Paridis Rhizoma
α-Spinasterol		2	0.00112741	0.296517413	2168	0.46	Codonopsis Radix Bupleuri Radix
β-Sitosterol		4	0.001437489	0.284622732	1380	0.435	Citri Reticulatae Pericarpium Astragali Radix Coicis Semen Clematidis Armandii Caulis
Palmitic Acid		3	0.004500068	0.314014752	6916	0.391	Codonopsis Radix Poria Bupleuri Radix
Stearic Acid		2	0.001096527	0.298298298	2304	0.322	Bupleuri Radix Coicis Semen
D-(−)-Fructose		2	2.53E-04	0.27618165	408	0.31	Codonopsis Radix Atractylodis Macrocephalae Rhizoma

GEHAT: GFL-efficacy group-herbal medicine-active compound-key target.

proteins ($P < 0.05$) and downregulated PIK3CG and PRKACA ($P < 0.05$). On the other hand, GFL-HD did not significantly affect the expression of these four target proteins ($P > 0.05$). These findings suggest that GFL-LD treatment can modulate the expression levels of key target proteins involved in lipid metabolism and apoptotic pathways in NAFLD rats (Fig. 11A and B).

4. Discussion

4.1. The impact of multi-component, multi-target strategies on NALFD

NAFLD, characterized by ≥ 5 % fat droplets in liver cells, with or without inflammation and necrosis, can be effectively treated by developing a drug with a multi-target, multi-component and multi-pathway strategy [21]. TCM employs Chinese herbal medicines and formulas to treat different syndrome types based on TCM syndrome differentiation [22]. These consisting of multiple drugs, possessing the characteristics of multi-component, multi-target and multi-pathway actions. Consequently, they can simultaneously target multiple pathological processes, regulate diverse signaling pathways and deliver several biological effects [23]. Chinese herbal formulas can offer an advantage in NAFLD treatment due to its complexity and it ability to counteract lipid metabolism disorder, oxidative stress, inflammatory response and liver fibrosis [24].
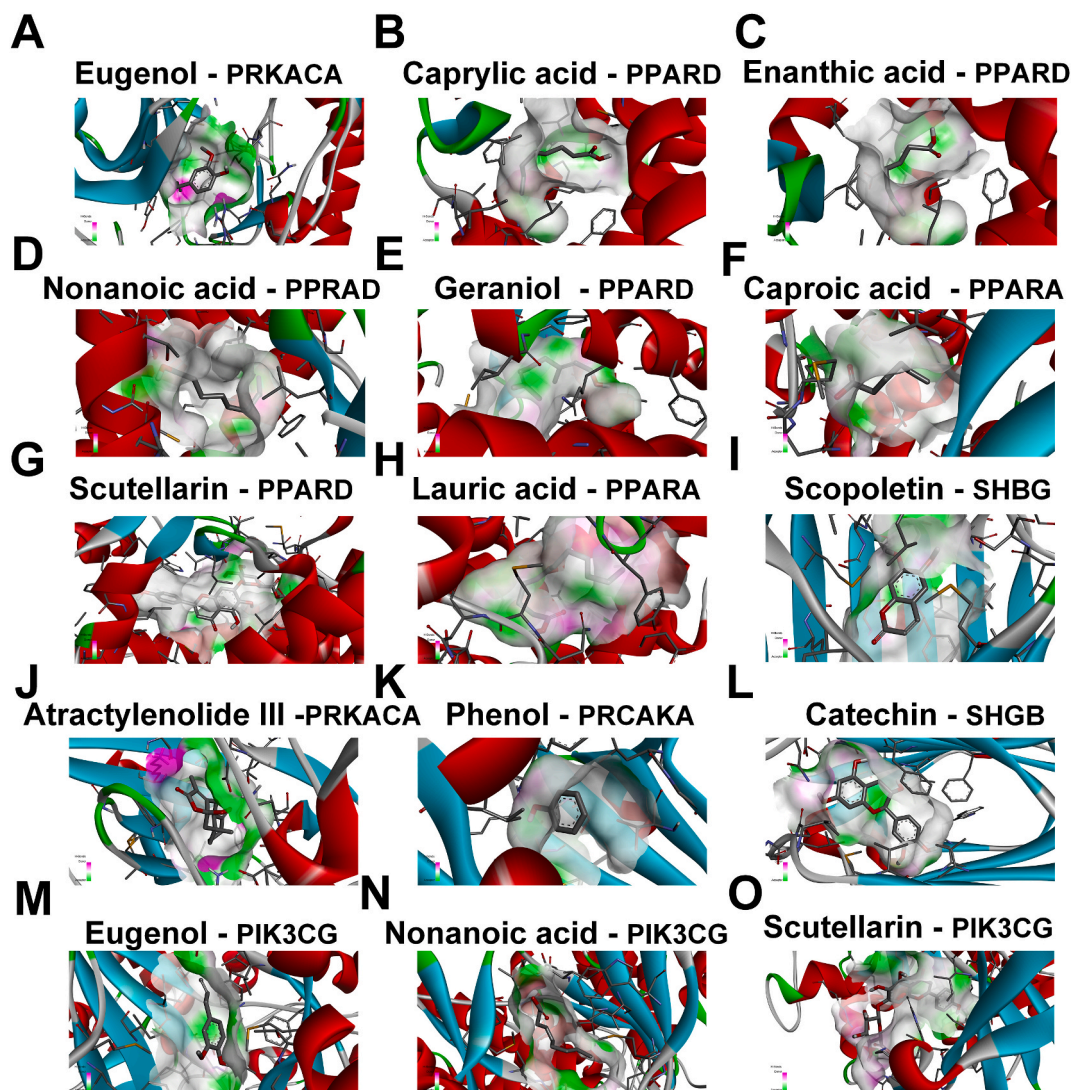
Fig. 6. (A–O) The three-dimensional molecular docking of the 13 core compounds of GFL in the treatment of NAFLD with their respective 5 core target proteins. The filtering criteria used were a Druglikeness Score ≥ 0.5 and a binding energy ≤ -4.25 kcal mol.

4.2. Active chemical component screening of GFL

In our preliminary study, we identified 78 chemical components in GFL through UPLC-Q-TOF/MS, which were primarily phenylpropanoids, flavonoids, anthraquinones, alkaloids, and terpenoids [12]. Phenolic compounds in plants are known to lower the risks linked to metabolic syndrome and type 2 diabetes [25]. Specifically, flavonoids and phenolic acids show antioxidant, anti-lipoxygenase, and anticancer properties. Anthraquinones also demonstrate anti-inflammatory, immunomodulatory, lipid-lowering, and anticancer effects [26–28].

GFL, which is rich in these components, aligns with the TCM theory of "spleen-invigorating and qi-regulating" treatments proven beneficial in NAFLD patients, improving liver function, blood sugar, and lipid levels [29]. Key medicinal herbs in GFL, such as Codonopsis Radix, Poria, and Astragali Radix, exhibit immunomodulatory effects, which are crucial in preventing NAFLD progression [30–34]. Additionally, Artemisiae Scopariae Herba and Aquilariae Lignum Resinatum, which the core components of GFL, offer anti-inflammatory, antioxidant, anti-fibrosis, and antitumor activities [35,36]. Furthermore, unsaturated fatty acids such as caproic and lauric acids in GFL can decrease liver fat and aid in regulating insulin resistance in NAFLD patients [37,38]. Other active ingredients, including eugenol, geraniol, scutellarin, and atractylenolide III, contribute to GFL's therapeutic effects via their antioxidant, anti-inflammatory, and antitumor properties [39–42]. Compounds including scopoletin and catechin further enhance GFL's benefits with their antioxidant, anti-inflammatory, antibacterial, and antitumor activities [43]. Therefore, GFL's chemical components synergistically contribute to its therapeutic effects in NAFLD treatment, aligning with the theoretical basis of TCM as well as modern biomedical understanding.
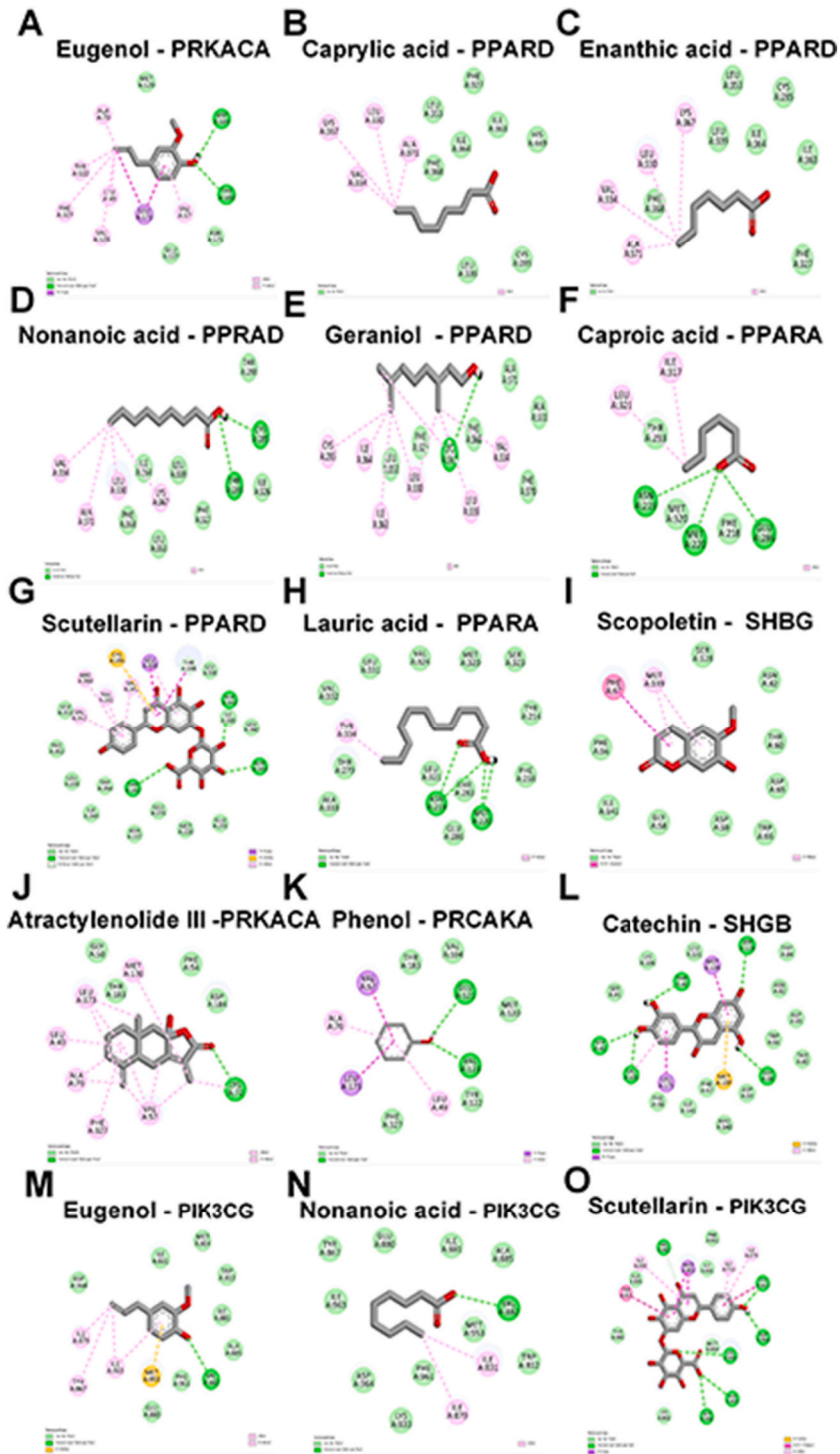
Fig. 7. The two-dimensional molecular docking between the 13 core compounds of GFL and the 5 core target proteins in the treatment of NAFLD. (A–O) The shallow green dashed lines indicate van der Waals interactions between the compounds and the surrounding amino acid residues. The deep green dashed lines represent hydrogen bond interactions between the compounds and the surrounding amino acid residues. The deep purple dashed lines indicate pi-sigma interactions between the compounds and the surrounding amino acid residues. The light pink dashed lines represent pi-alkyl interactions between the compounds and the surrounding amino acid residues. The ocher dashed lines represent pi-sulfur interactions between the compounds and the surrounding amino acid residues. These interactions play crucial roles in determining the binding affinities and specificities of the compounds to their target proteins. The different types of interactions contribute to the overall stability and conformation of the compound-protein complexes, influencing their functional outcomes in the treatment of NAFLD.
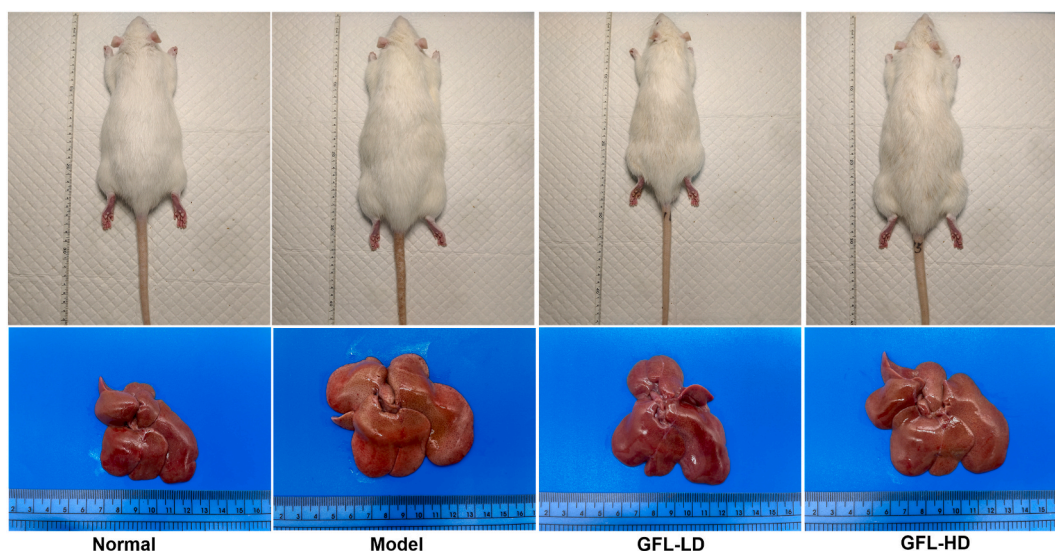
Fig. 8. A comparison of the external appearance and liver condition of rats in the GFL-LD, GFL-HD, Normal and Model groups before and after treatment with GFL.

4.3. Analysis of the core nodes in complex network and functional enrichment

Our study identified 28 NAFLD-related target genes that overlap with GFL targets, highlighting their potential importance in NAFLD treatment. PPI network analysis pinpointed key genes such as PPARA, PPARD, PRKACA and PIK3CG which are essential in lipid metabolism, apoptosis, and inflammation. These genes, expressed in the liver and immune cells, emerge as promising targets for GFL therapy in NAFLD. We also explored a complex TCM formula of 18 herbs using a network pharmacology approach. This led to the identification of 19 core chemical components and 13 key protein targets linked to NAFLD. Herbs like Rhei Radix et Rhizoma, Poria, Bupleuri Radix, Astragali Radix, Codonopsis Radix, Aquilariae Lignum Resinatum and Artemisiae Scopariae Herba were found to play a central role in NAFLD treatment.

Molecular docking analysis confirmed the strong binding between these herbal components and key protein targets, shedding light on the molecular mechanisms underlying the formula's therapeutic effects. Specifically, compounds such as eugenol, nonanoic acid, geraniol, lauric acid, scutellarin, catechin, and atractylenolide III exhibit strong binding affinities for PPARA, PPARD, PRKACA, PIK3CG, and SHBG, which are crucial targets in the pathogenesis of NAFLD. Notably, the molecular docking results provided insights into the types of intermolecular forces at play in these interactions. The identified forces, including van der Waals interactions, hydrogen bonds, pi-sigma, pi-alkyl and pi-sulfur interactions, are known to contribute significantly to molecule recognition and their binding specificities. For instance, van der Waals forces, which arise from temporary dipoles induced by fluctuations in electron distributions, are crucial for stabilizing molecule-target complexes [44]. Hydrogen bonding, a stronger intermolecular force, often determines the specificity and stability of ligand-receptor interactions [45].The pi-interactions which were identified in our study are also essential for molecular recognition, particularly in aromatic systems [46]. These interactions, though weaker than hydrogen bonds, can contribute to the binding affinity and specificity of herbal compounds to their targets. These molecular interactions are potentially key in regulating lipid metabolism, insulin sensitivity, and inflammatory responses, of which are critical processes in NAFLD pathophysiology. Understanding these interactions provides deeper insights into how the identified TCM components exert their therapeutic effects.

4.4. Possible cellular and molecular mechanisms of GFL against NAFLD

We used rats fed with a high-fat diet and measured indicators such as serum TC, TG, ALT, AST, LDL-C and HDL-C which reflect the metabolic status and liver damage in NAFLD rats. When comparing these indicators between different groups of rats, we found that GFL treatment effectively improved liver function and blood lipid indicators. Histopathological examination of liver tissue further revealed improvements in liver weight index, reduction in hepatocellular steatosis and improved liver tissue structure, indicating that a low dose of GFL was able to alleviate NAFLD-related pathological changes.

PPARA and PPARD are nuclear receptors involved in regulating lipid metabolism, glucose metabolism and inflammatory response. Recent studies suggest that they also influence cell apoptosis by regulating various proteins and signaling pathways associated with apoptosis [47–49]. Downregulation of PPARA and PPARD has been observed in liver cancer, resulting in reduced cell apoptosis and increased proliferation of tumor cells and these two receptors were shown to be potential targets for GFL in this study. PIK3CG (also known as PI3Kγ) signaling plays a crucial role in regulating metabolic and inflammatory stress, and it is a potential target for therapeutic interventions in metabolic diseases, inflammation, and cardiovascular disorders [50]. Inhibition of PIK3CG has shown promise
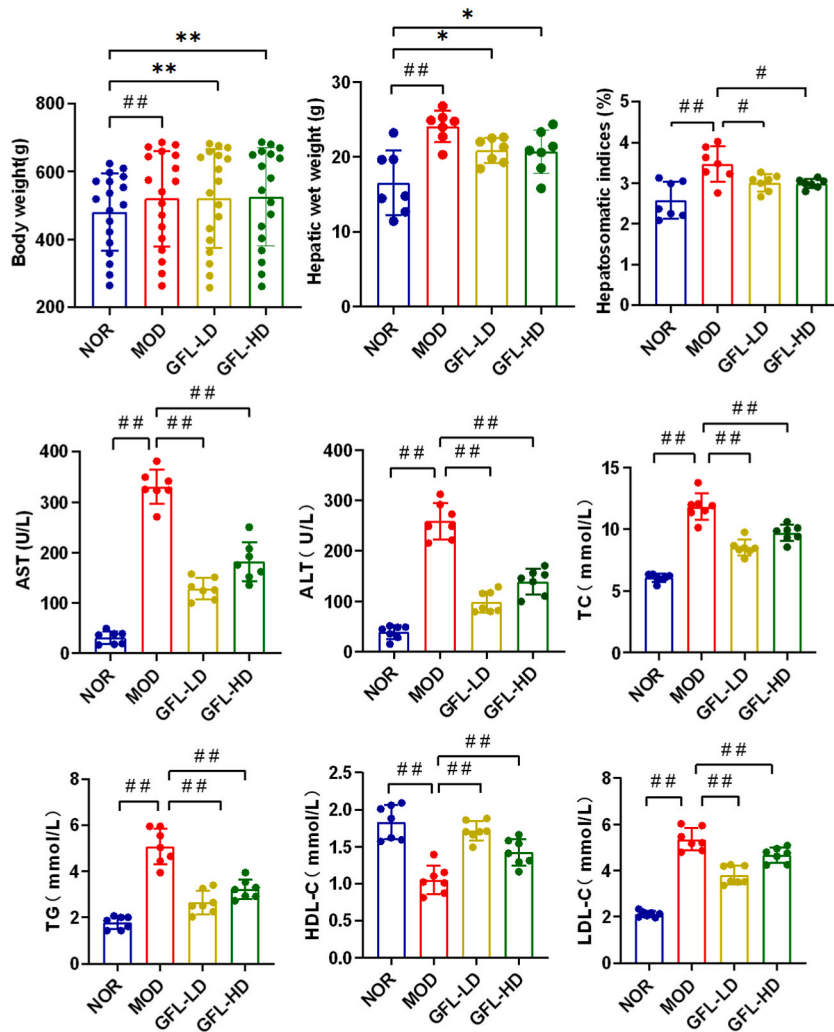
Fig. 9. The effects of GFL on liver morphology and blood lipid levels in rats with NAFLD. The Figures provide evidence that GFL treatment leads to improvements in liver morphology and blood lipid levels in NAFLD rats.

Notes: In comparison to the MOD group, the symbols #, and ## indicate significant differences of $P < 0.05$, $P < 0.01$, respectively. In comparison to the NOR group, symbols (* and **) indicate significant differences of $P < 0.05$ and $P < 0.01$, respectively.

in the treatment of human B-cell malignancies and this has been approved for clinical use. Consequently, it represents a potential therapeutic approach for hepatocellular carcinoma cells (HCC) [51,52]. The fusion of PRKACA and DNAJ homolog subfamily B member 1 is recognized as a potential utility of kinase inhibitors, targeting candidate biomarkers and therapeutic targets for fibrolamellar HCC [53–55]. Recent evidence suggests that NAFLD is a leading cause of HCC in the USA [56]. Regulation of PRKACA may potentially restore hepatic lipid homeostasis, improve metabolic dysregulation and attenuate the detrimental effects of inflammation in NAFLD. Analysis of GFL's effects on target proteins revealed significant alterations in the expression levels of PPARA, PPARD, PIK3CG and PRKACA in NAFLD rats. Low doses of GFL was found to modulate these target proteins. These findings demonstrate GFL's ability to regulate key proteins involved in lipid metabolism and apoptosis pathways in NAFLD.

5. Limitation and future perspectives

GCs, a renowned TCM formula, have been clinically applied in China for over 20 years, with widely recognized safety and efficacy. Our study integrated bioinformatics analysis with animal experiments to probe the mechanisms of GCs, focusing primarily on the 18 plant-based medicinal components. However, we recognize that GCs also contain 3 animal-based ingredients, which were not included in the initial bioinformatics analysis due to limited data on macromolecular animal proteins in authoritative databases such as TCMIP and ETCM. The proportion of the 18 herbs in GFL is 85.7 % (CNKI (https://www.cnki.net). Based on this database and other authoritative Chinese herbal medicine sources, the chemical components of the three animal-derived medicines in GFL are mainly, amino acids, peptides and proteins which would be readily digested to smaller components before entering the body. There are no
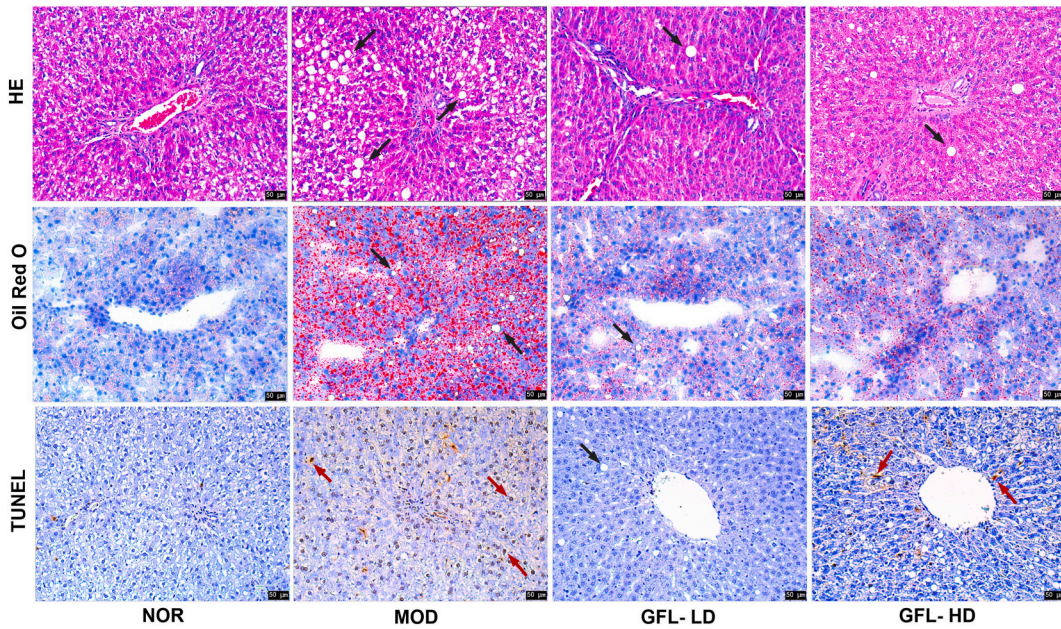
Fig. 10. The effects of GFL on improving the histological characteristics of NAFLD in rat liver tissues. In the HE-stained images (first row), the black arrows indicate the presence of fat droplets in the liver tissue, highlighting the characteristic features of NAFLD. In the oil red O-stained images (second row), black arrows also point to the accumulation of lipid droplets in the liver tissue, further confirming the presence of steatosis. The TUNEL-stained images (third row) show red arrows, indicating apoptotic cells in the liver tissue. The scale bar in the images represents a length of 50 μm, and the magnification used for capturing the images was 200 times.
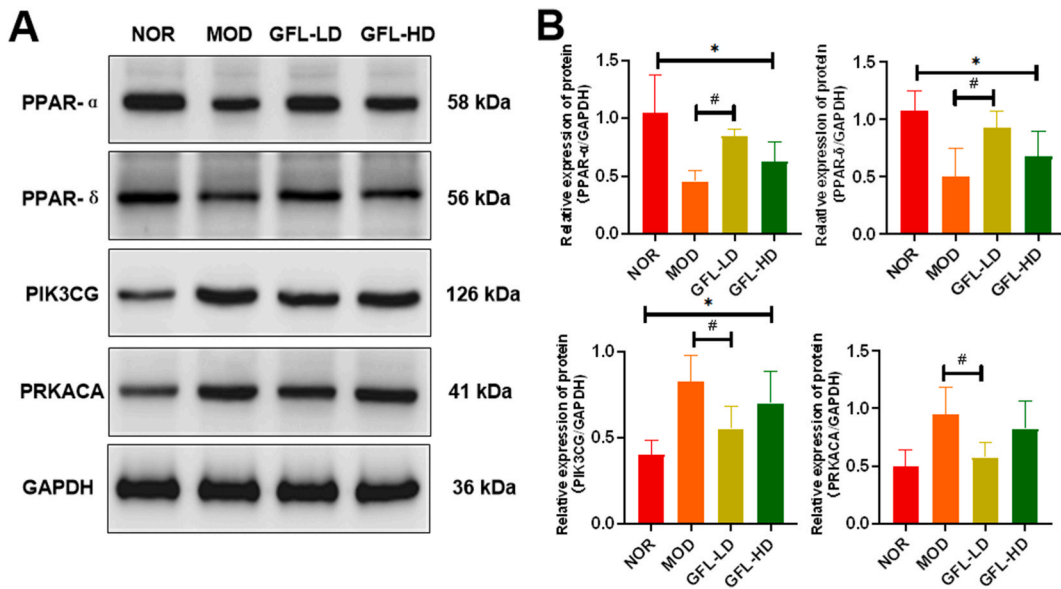

Fig. 11. The effects of GFL on key target proteins in rats with NAFLD was evaluated using western blotting. (A–B) The relative expression levels of target proteins PPARA, PPARD, PIK3CG and PRKACA were quantified.
Notes: # represent $P < 0.05$, when comparing the GFL-treated group to the MOD group. * represent $P < 0.05$, when compared to the NOR group.

major specific components to account for GFL's treatment of fatty liver disease.

In future studies, a refinement of refining multi-component herbal medications to the use of nanoparticles may offer immense potential in enhancing solubility, targeting, stability, and bioavailability, thereby their boosting therapeutic efficacy [57,58]. These novel cutting-edge technologies will provide more efficient and safer drug delivery methods. Our approach allowed insights into potential targets and pathways modulated by the herbal components. However, there are limitations, primarily related to the

incomplete understanding of the role of animal-based components. Future research should aim to fill this gap by exploring additional databases, targeted experiments on animal-derived ingredients and funding large scale randomized clinical trials on the use of GCs.

Moreover, while our study provides valuable insights, clinical trials are necessary to evaluate GCs' safety and efficacy in human subjects with NAFLD, which should focus on the optimal dosage to use, treatment duration, and potential side-effects. The long-term effects of GCs and its impact on disease progression and metabolic parameters also warrant investigation. Future NAFLD treatment strategies should be precise and personalized, exploring new targets and drugs such as inhibitors and agonists which target specific pathways. Additionally, strengthening research on the interaction mechanisms between hepatocyte apoptosis and other cell death modalities are crucial for a more comprehensive NAFLD intervention and treatment strategy.

6. Conclusions

Our study demonstrates that GCs are effective in improving the pathological changes associated with NAFLD in a high-fat diet-induced rat model. They can reduces fat deposition, improves blood lipid indicators and modulates the expression levels of key target proteins, including PPARA, PPARD, PIK3CG and PRKACA, which are involved in lipid metabolism and the apoptosis pathways in NAFLD. These effects help to prevent subsequent liver cell damage and maintain the normal physiological functions of lipid metabolism in the liver. Overall, our findings enhance the understanding of GFL's therapeutic potential in NAFLD treatment and lay the groundwork for future research and its clinical applications.

Funding

Data availability statement

The original experimental data involved in this study, due to containing traditional craftsmanship protection and copyright protection information, cannot be publicly accessed. The datasets used and analyzed during the current study are available from the corresponding author on reasonable request.

Ethics statement

The animal experiments were reviewed and approved by the Animal Ethics Committee of Wuhan Myhalic Biotechnology Co., Ltd. (Wuhan, China; Approval number:HLK-20210315-001).

CRediT authorship contribution statement

Yu Pan: Writing – review & editing, Writing – original draft, Visualization, Validation, Methodology, Investigation, Funding acquisition, Data curation, Conceptualization. **Liya Qiao:** Resources, Methodology, Investigation, Data curation. **Yunkun Zhang:** Validation, Resources, Methodology, Investigation, Funding acquisition, Data curation. **Suren R. Sooranna:** Writing – review & editing, Conceptualization. **Danna Huang:** Validation, Resources, Methodology, Investigation. **Min Ou:** Validation, Methodology. **Fei Xu:** Writing – review & editing, Supervision, Resources, Funding acquisition. **Lu Chen:** Writing – review & editing, Supervision. **Dan Huang:** Writing – review & editing, Supervision.

Declaration of competing interest

The authors declare that they have no known competing financial interests or personal relationships that could have appeared to influence the work reported in this paper.

Appendix A. Supplementary data

Supplementary data to this article can be found online at https://doi.org/10.1016/j.heliyon.2024.e34297.

References

[1] N. Chalasani, Z. Younossi, J.E. Lavine, et al., The diagnosis and management of nonalcoholic fatty liver disease: practice guidance from the American Association for the Study of Liver Diseases, Hepatology 67 (1) (2018) 328–357, https://doi.org/10.1002/hep.29367.

[2] Z.M. Younossi, P. Golabi, L. de Avila, et al., The global epidemiology of NAFLD and NASH in patients with type 2 diabetes: a systematic review and meta-analysis, J. Hepatol. 71 (4) (2019) 793–801, https://doi.org/10.1016/j.jhep.2019.06.021.

[3] C. Estes, Q.M. Anstee, M.T. Arias-Loste, et al., Modeling NAFLD disease burden in China, France, Germany, Italy, Japan, Spain, United Kingdom, and United States for the period 2016-2030, J. Hepatol. 69 (4) (2018) 896–904, https://doi.org/10.1016/j.jhep.2018.05.036.

[4] Z.M. Younossi, D. Blissett, R. Blissett, et al., The economic and clinical burden of nonalcoholic fatty liver disease in the United States and Europe, Hepatology 64 (5) (2016) 1577–1586, https://doi.org/10.1002/hep.28785.

[5] X. Dai, J. Feng, Y. Chen, et al., Traditional Chinese Medicine in nonalcoholic fatty liver disease: molecular insights and therapeutic perspectives, Chin. Med. 16 (1) (2021) 68, https://doi.org/10.1186/s13020-021-00469-4. Published 2021 Aug 3.

[6] H. Zhou, C. Ma, C. Wang, L. Gong, Y. Zhang, Y. Li, Research progress in use of traditional Chinese medicine monomer for treatment of non-alcoholic fatty liver disease, Eur. J. Pharmacol. 898 (2021) 173976, https://doi.org/10.1016/j.ejphar.2021.173976.

[7] M. Chen, Y. Xie, S. Gong, et al., Traditional Chinese medicine in the treatment of nonalcoholic steatohepatitis, Pharmacol. Res. 172 (2021) 105849, https://doi.org/10.1016/j.phrs.2021.105849.

[8] Y. Xu, W. Guo, C. Zhang, et al., Herbal medicine in the treatment of non-alcoholic fatty liver diseases-efficacy, action mechanism, and clinical application, Front. Pharmacol. 11 (2020) 601, https://doi.org/10.3389/fphar.2020.00601. Published 2020 May 12.

[9] C. Ke, J. Gao, J. Tu, et al., Ganfule capsule alleviates bile duct ligation-induced liver fibrosis in mice by inhibiting glutamine metabolism, Front. Pharmacol. 13 (2022) 930785, https://doi.org/10.3389/fphar.2022.930785. Published 2022 Oct 7.

[10] K. Li, K. Xiao, S. Zhu, Y. Wang, W. Wang, Chinese herbal medicine for primary liver cancer therapy: perspectives and challenges, Front. Pharmacol. 13 (2022) 889799, https://doi.org/10.3389/fphar.2022.889799. Published 2022 May 5.

[11] F. Xu, H. Li, Y. Pan, et al., Effects of Ganfule capsule on microbial and metabolic profiles in anti-hepatocellular carcinoma, J. Appl. Microbiol. 132 (3) (2022) 2280–2292, https://doi.org/10.1111/jam.15307.

[12] X.U. Fei, Yu Pan, L.I. Han-ying, et al., Identification of chemical constituents in Ganfule by UPLC-Q-TOF/MS combined with UNIFI software, Chin J Pharm Anal (药物分析杂志) 41 (5) (2021) 760–778, https://doi.org/10.16155/j.0254-1793.2021.05.03.

[13] A.L. Hopkins, Network pharmacology: the next paradigm in drug discovery, Nat. Chem. Biol. 4 (11) (2008) 682–690, https://doi.org/10.1038/nchembio.118.

[14] C. Nogales, Z.M. Mamdouh, M. List, C. Kiel, A.I. Casas, H.H.H.W. Schmidt, Network pharmacology: curing causal mechanisms instead of treating symptoms, Trends Pharmacol. Sci. 43 (2) (2022) 136–150, https://doi.org/10.1016/j.tips.2021.11.004.

[15] L. Pinzi, G. Rastelli, Molecular docking: shifting paradigms in drug discovery, Int. J. Mol. Sci. 20 (18) (2019) 4331, https://doi.org/10.3390/ijms20184331. Published 2019 Sep. 4.

[16] X. Wang, Y. Shen, S. Wang, et al., PharmMapper 2017 update: a web server for potential drug target identification with a comprehensive target pharmacophore database, Nucleic Acids Res. 45 (W1) (2017) W356–W360, https://doi.org/10.1093/nar/gkx374.

[17] H. Xu, Y. Zhang, P. Wang, et al., A comprehensive review of integrative pharmacology-based investigation: a paradigm shift in traditional Chinese medicine, Acta Pharm. Sin. B 11 (6) (2021) 1379–1399, https://doi.org/10.1016/j.apsb.2021.03.024.

[18] F. Kalhori, H. Yazdyani, F. Khademorezaeian, et al., Enzyme activity inhibition properties of new cellulose nanocrystals from Citrus medica L. pericarp: a perspective of cholesterol lowering, Luminescence 37 (11) (2022) 1836–1845, https://doi.org/10.1002/bio.4360.

[19] A. Sharifi-Rad, J. Mehrzad, M. Darroudi, M.R. Saberi, J. Chamani, Oil-in-water nanoemulsions comprising Berberine in olive oil: biological activities, binding mechanisms to human serum albumin or holo-transferrin and QMMD simulations, J. Biomol. Struct. Dyn. 39 (3) (2021) 1029–1043, https://doi.org/10.1080/07391102.2020.1724568.

[20] G. Heinzelmann, M.K. Gilson, Automation of absolute protein-ligand binding free energy calculations for docking refinement and compound evaluation, Sci. Rep. 11 (1) (2021) 1116, https://doi.org/10.1038/s41598-020-80769-1. Published 2021 Jan 13.

[21] C.D. Byrne, G. Targher, NAFLD: a multisystem disease, J. Hepatol. 62 (1 Suppl) (2015) S47–S64, https://doi.org/10.1016/j.jhep.2014.12.012.

[22] Y. Liu, S. Yang, K. Wang, et al., Cellular senescence and cancer: focusing on traditional Chinese medicine and natural products, Cell Prolif. 53 (10) (2020) e12894, https://doi.org/10.1111/cpr.12894.

[23] H. Li, Advances in anti hepatic fibrotic therapy with Traditional Chinese Medicine herbal formula, J. Ethnopharmacol. 251 (2020) 112442, https://doi.org/10.1016/j.jep.2019.112442.

[24] H. Yao, Y.J. Qiao, Y.L. Zhao, et al., Herbal medicines and nonalcoholic fatty liver disease, World J. Gastroenterol. 22 (30) (2016) 6890–6905, https://doi.org/10.3748/wjg.v22.i30.6890.

[25] K. Kasprzak-Drozd, T. Oniszczuk, M. Stasiak, A. Oniszczuk, Beneficial effects of phenolic compounds on gut microbiota and metabolic syndrome, Int. J. Mol. Sci. 22 (7) (2021) 3715, https://doi.org/10.3390/ijms22073715. Published 2021 Apr 2.

[26] Q. Wang, Y. Ou, G. Hu, et al., Naringenin attenuates non-alcoholic fatty liver disease by down-regulating the NLRP3/NF-κB pathway in mice, Br. J. Pharmacol. 177 (8) (2020) 1806–1821, https://doi.org/10.1111/bph.14938.

[27] M. Imran, A. Rauf, T. Abu-Izneid, et al., Luteolin, a flavonoid, as an anticancer agent: a review [published correction appears in Biomed Pharmacother. 2019 Aug;116:109084], Biomed. Pharmacother. 112 (2019) 108612, https://doi.org/10.1016/j.biopha.2019.108612.

[28] L. Dong, H. Du, M. Zhang, et al., Anti-inflammatory effect of Rhein on ulcerative colitis via inhibiting PI3K/Akt/mTOR signaling pathway and regulating gut microbiota, Phytother Res. 36 (5) (2022) 2081–2094, https://doi.org/10.1002/ptr.7429.

[29] X. Li, X. Hu, T. Pan, et al., Kanglexin, a new anthraquinone compound, attenuates lipid accumulation by activating the AMPK/SREBP-2/PCSK9/LDLR signalling pathway, Biomed. Pharmacother. 133 (2021) 110802, https://doi.org/10.1016/j.biopha.2020.110802.

[30] W. Wang, A.L. Xu, Z.C. Li, et al., Combination of probiotics and salvia miltiorrhiza polysaccharide alleviates hepatic steatosis via gut microbiota modulation and insulin resistance improvement in high fat-induced NAFLD mice, Diabetes Metab. J 44 (2) (2020) 336–348, https://doi.org/10.4093/dmj.2019.0042.

[31] H. Ye, S. Ma, Z. Qiu, et al., Poria cocos polysaccharides rescue pyroptosis-driven gut vascular barrier disruption in order to alleviates non-alcoholic steatohepatitis, J. Ethnopharmacol. 296 (2022) 115457, https://doi.org/10.1016/j.jep.2022.115457.

[32] H. Ye, S. Ma, Z. Qiu, et al., Poria cocos polysaccharides rescue pyroptosis-driven gut vascular barrier disruption in order to alleviates non-alcoholic steatohepatitis, J. Ethnopharmacol. 296 (2022) 115457, https://doi.org/10.1016/j.jep.2022.115457.

[33] S. Lei, S. Zhao, X. Huang, et al., Chaihu Shugan powder alleviates liver inflammation and hepatic steatosis in NAFLD mice: a network pharmacology study and in vivo experimental validation, Front. Pharmacol. 13 (2022) 967623, https://doi.org/10.3389/fphar.2022.967623. Published 2022 Sep. 12.

[34] Y. Zhang, K. Tang, Y. Deng, et al., Effects of shenling baizhu powder herbal formula on intestinal microbiota in high-fat diet-induced NAFLD rats, Biomed. Pharmacother. 102 (2018) 1025–1036, https://doi.org/10.1016/j.biopha.2018.03.158.

[35] F.F. Cai, Y.Q. Bian, R. Wu, et al., Yinchenhao decoction suppresses rat liver fibrosis involved in an apoptosis regulation mechanism based on network pharmacology and transcriptomic analysis, Biomed. Pharmacother. 114 (2019) 108863, https://doi.org/10.1016/j.biopha.2019.108863.

[36] X. Zhang, Z. Zhang, P. Wang, et al., Bawei Chenxiang wan ameliorates cardiac hypertrophy by activating AMPK/PPAR-α signaling pathway improving energy metabolism, Front. Pharmacol. 12 (2021) 653901, https://doi.org/10.3389/fphar.2021.653901. Published 2021 Jun 3.

[37] G. Zhao, L. Yang, W. Zhong, et al., Polydatin, A glycoside of resveratrol, is better than resveratrol in alleviating non-alcoholic fatty liver disease in mice fed a high-fructose diet, Front. Nutr. 9 (2022) 857879, https://doi.org/10.3389/fnut.2022.857879. Published 2022 May 16.

[38] V. Saraswathi, N. Kumar, T. Gopal, et al., Lauric acid versus palmitic acid: effects on adipose tissue inflammation, insulin resistance, and non-alcoholic fatty liver disease in obesity, Biology 9 (11) (2020) 346, https://doi.org/10.3390/biology9110346. Published 2020 Oct 22.

[39] M. Ulanowska, B. Olas, Biological properties and prospects for the application of eugenol-A review, Int. J. Mol. Sci. 22 (7) (2021) 3671, https://doi.org/10.3390/ijms22073671. Published 2021 Apr 1.

[40] J. Chen, X. Fan, L. Zhou, X. Gao, Treatment with geraniol ameliorates methionine-choline-deficient diet-induced non-alcoholic steatohepatitis in rats, J. Gastroenterol. Hepatol. 31 (7) (2016) 1357–1365, https://doi.org/10.1111/jgh.13272.

[41] X. Zhang, Z. Huo, H. Luan, et al., Scutellarin ameliorates hepatic lipid accumulation by enhancing autophagy and suppressing IRE1α/XBP1 pathway, Phytother Res. 36 (1) (2022) 433–447, https://doi.org/10.1002/ptr.7344.

[42] Q. Li, J.X. Tan, J. He, et al., Atractylenolide III ameliorates non-alcoholic fatty liver disease by activating hepatic adiponectin receptor 1-mediated AMPK pathway, Int. J. Biol. Sci. 18 (4) (2022) 1594–1611, https://doi.org/10.7150/ijbs.68873. Published 2022 Jan 31.

[43] U. Shabbir, M. Rubab, E.B. Daliri, R. Chelliah, A. Javed, D.H. Oh, Curcumin, quercetin, catechins and metabolic diseases: the role of gut microbiota, Nutrients 13 (1) (2021) 206, https://doi.org/10.3390/nu13010206. Published 2021 Jan 12.

[44] A.S. Dimitrov, Methods in molecular biology. Therapeutic antibodies. Methods and protocols. Preface, Methods Mol. Biol. 525 (2009), https://doi.org/10.1007/978-1-59745-554-1 vii-xiii.

[45] D. Chen, N. Oezguen, P. Urvil, C. Ferguson, S.M. Dann, T.C. Savidge, Regulation of protein-ligand binding affinity by hydrogen bond pairing, Sci. Adv. 2 (3) (2016) e1501240, https://doi.org/10.1126/sciadv.1501240. Published 2016 Mar 25.

[46] Z. Liang, Q.X. Li, π-Cation interactions in molecular recognition: perspectives on pharmaceuticals and pesticides, J. Agric. Food Chem. 66 (13) (2018) 3315–3323, https://doi.org/10.1021/acs.jafc.8b00758.

[47] T. Yan, Y. Luo, N. Yan, et al., Intestinal peroxisome proliferator-activated receptor α-fatty acid-binding protein 1 axis modulates nonalcoholic steatohepatitis, Hepatology 77 (1) (2023) 239–255, https://doi.org/10.1002/hep.32538.

[48] M. Pawlak, P. Lefebvre, B. Staels, Molecular mechanism of PPARα action and its impact on lipid metabolism, inflammation and fibrosis in non-alcoholic fatty liver disease, J. Hepatol. 62 (3) (2015) 720–733, https://doi.org/10.1016/j.jhep.2014.10.039.

[49] M. Zarei, D. Aguilar-Recarte, X. Palomer, M. Vázquez-Carrera, Revealing the role of peroxisome proliferator-activated receptor β/δ in nonalcoholic fatty liver disease, Metabolism 114 (2021) 154342, https://doi.org/10.1016/j.metabol.2020.154342.

[50] W. Zhang, Y. Liu, M. Wu, et al., PI3K inhibition protects mice from NAFLD by down-regulating CMKLR1 and NLRP3 in Kupffer cells, J. Physiol. Biochem. 73 (4) (2017) 583–594, https://doi.org/10.1007/s13105-017-0589-6.

[51] M.P. Wymann, G. Solinas, Inhibition of phosphoinositide 3-kinase γ attenuates inflammation, obesity, and cardiovascular risk factors, Ann. N. Y. Acad. Sci. 1280 (2013) 44–47, https://doi.org/10.1111/nyas.12037.

[52] E. Ko, H.W. Seo, E.S. Jung, et al., PI3Kδ is a therapeutic target in hepatocellular carcinoma, Hepatology 68 (6) (2018) 2285–2300, https://doi.org/10.1002/hep.30307.

[53] Lola Reid, Praveen Sethupathy, The DNAJB1-PRKACA chimera: candidate biomarker and therapeutic target for fibrolamellar carcinomas, Hepatology 63 (2) (February 2016) 662–664, https://doi.org/10.1002/hep.28307.

[54] S. Gao, H. Tan, D. Li, Oridonin suppresses gastric cancer SGC-7901 cell proliferation by targeting the TNF-alpha/androgen receptor/TGF-beta signalling pathway axis, J. Cell Mol. Med. 27 (18) (2023 Sep) 2661–2674, https://doi.org/10.1111/jcmm.17841. Epub 2023 Jul 11. PMID: 37431884; PMCID: PMC10494293.

[55] S. Gao, J. Gang, M. Yu, G. Xin, H. Tan, Computational analysis for identification of early diagnostic biomarkers and prognostic biomarkers of liver cancer based on GEO and TCGA databases and studies on pathways and biological functions affecting the survival time of liver cancer, BMC Cancer 21 (1) (2021 Jul 8) 791, https://doi.org/10.1186/s12885-021-08520-1. PMID: 34238253; PMCID: PMC8268589.

[56] D.Q. Huang, H.B. El-Serag, R. Loomba, Global epidemiology of NAFLD-related HCC: trends, predictions, risk factors and prevention, Nat. Rev. Gastroenterol. Hepatol. 18 (2021) 223–238, https://doi.org/10.1038/s41575-020-00381-6.

[57] M. Kaffash, S. Tolou-Shikhzadeh-Yazdi, S. Soleimani, S. Hoseinpoor, M.R. Saberi, J. Chamani, Spectroscopy and molecular simulation on the interaction of Nano-Kaempferol prepared by oil-in-water with two carrier proteins: an investigation of protein-protein interaction, Spectrochim. Acta Mol. Biomol. Spectrosc. 309 (2024) 123815, https://doi.org/10.1016/j.saa.2023.123815.

[58] Maheri Hamid, Fatemeh Hashemzadeh, Niloofar Shakibapour, Elahe Kamelniya, Bizhan Malaekeh-Nikouei, Parisa Mokaberi, Jamshidkhan Chamani, Glucokinase activity enhancement by cellulose nanocrystals isolated from jujube seed: a novel perspective for type II diabetes mellitus treatment (In vitro), J. Mol. Struct. 1269 (2022) 133803, https://doi.org/10.1016/j.molstruc.2022.133803.